processes

MDPI

Article

Supercritical Carbon Dioxide Cycles for Concentrated Solar Power Plants: A Possible Alternative for Solar Desalination

Rafael González-Almenara, Pablo Rodríguez de Arriba, Francesco Crespi, David Sánchez *, Antonio Muñoz and Tomás Sánchez-Lencero

Department of Energy Engineering, University of Seville, ETSI, Camino de los Descubrimientos, s/n, 41092 Seville, Spain; rgalmenara@us.es (R.G.-A.); prdearriba@us.es (P.R.d.A.); crespi@us.es (F.C.); ambl@us.es (A.M.); tmsl@us.es (T.S.-L.)

* Correspondence: ds@us.es

Abstract: This manuscript investigates the supercritical carbon dioxide (sCO_2) power cycle employed in the power block of concentrated solar power (CSP) plants—solar tower—as an alternative for solar desalination, developed with either distillation or reverse osmosis. This concept is investigated as a possible up-scaling of the SOLMIDEFF project, originally based on a hot-air micro gas turbine combined with a solar dish collector. For the upscaled concept, five different sCO_2 cycles are considered, chosen amongst the best-performing configurations proposed in the literature for CSP applications, and modelled with Thermoflex software. The influence of ambient conditions is studied, considering two minimum cycle temperatures (35 °C and 50 °C), corresponding to *Santa Cruz de Tenerife* and *Abu Dhabi*, respectively. The results show that the low temperatures at the inlet of the heat rejection unit compromise the viability of distillation technologies. On the other hand, the high thermal efficiency achieved by these cycles, especially with the *recompression* and *partial cooling* layouts, reduces the specific energy consumption when combined with reverse osmosis (RO), below that of photovoltaic (PV)+RO. Feed-water preheating is explored as a solution to further reduce energy consumption, concluding that its actual interest is not clear and strongly depends on the location considered and the corresponding water quality standards.

Keywords: supercritical CO_2; concentrated solar power; solar desalination; reverse osmosis; supercritical carbon dioxide

Citation: González-Almenara, R.; Rodríguez de Arriba, P.; Crespi, F.; Sánchez, D.; Muñoz, A.; Sánchez-Lencero, T. Supercritical Carbon Dioxide Cycles for Concentrated Solar Power Plants: A Possible Alternative for Solar Desalination. *Processes* **2022**, *10*, 72. https://doi.org/10.3390/pr10010072

Academic Editors: Agustin M. Delgado-Torres and Lourdes García-Rodríguez

Received: 31 October 2021
Accepted: 24 December 2021
Published: 30 December 2021

1. Introduction

The supercritical CO_2 technology is currently living through times of flourishing interest in the scientific community. One proof of this is the vast growth in the number of research publications and patents, which have increased fivefold from 2010 to 2020 [1]. Another evidence of the potential of the sCO_2 technology is the rise in internationally funded projects on the topic, for example, the SCARABEUS [2], COMPASSCO2 [3], sCO2 Flex [4], sCO2-4-NPP [5], sCO_2-HeRo [6], I-ThERM [7] or CO2OLHEAT [8] projects, to name a few. Moreover, the number of technical meetings and conferences specific to sCO_2 technology has also risen. Examples are the *Supercritical CO_2 Power Cycles Symposium*, the *European sCO_2 Conference for Energy Systems* or the dedicated Technical Committee in the *ASME Turbo Expo* conference. All this interest is justified by the fact that sCO_2 power cycles are able to achieve high thermal efficiency (in excess of 50% for peak temperatures of around 700 °C) with simple and compact layouts, which translates into a lower footprint and higher operational flexibility than conventional power systems. Additionally, this technology is suitable for diverse applications, such as waste heat recovery, coal-fired plants, Gen IV nuclear reactors, concentrated solar power and oxy-combustion systems.

Bearing all this in mind, the present paper investigates a solar desalination concept, based on the combination of solar tower—employing supercritical carbon dioxide cycle in its power block—with either distillation or reverse osmosis. The first part of the paper

provides a brief introduction to the SOLMIDEFF concept, followed by a review of the recent history and the fundamentals of sCO_2 power cycles, together with a brief discussion regarding the feasibility of this technology when combined with CSP plants. Afterwards, the computational environment and the methodology employed in the analysis are presented, and the main results are discussed. Two different possible locations are considered—*Santa cruz de Tenerife* (Canary Islands, Spain) and *Abu Dhabi* (UAE)—standing for two different cycle minimum temperatures (35 °C and 50 °C, respectively). Moreover, two different turbine inlet temperatures are taken into account: 550 °C, corresponding to the state of the art of solar tower power plants, and 700 °C, representative of next generation CSP. Five different cycle layouts are proposed, selected among the most interesting ones found in literature, in order to identify the best candidate for this solar desalination concept for either distillation or reverse osmosis. Finally, the possibility to add the preheating process to the RO is analysed and discussed. The increasing demand in both energy and purified water as a consequence of the growth in the worldwide population is a major challenge posed to humankind in this decade. One environmentally friendly solution to potentially address this water–energy nexus problem is the integration of desalination with renewable energies, for example, solar desalination. A particularly interesting scenario is the one related to semi-arid regions, where concentrated solar power plants linked to reverse osmosis or any distillation (i.e., thermal desalination) process could address both needs [9]. In this context, the SOLMIDEFF project stands out as a very promising alternative, due to its compactness and high versatility [10] (more information in the next section). Nevertheless, an important drawback of SOLMIDEFF is the inherently small scale brought about by the solar energy collection (parabolic dish) and power conversion (micro gas turbine) systems (<50 kWe), which make it difficult to upscale the system to much larger power and water productions. Accordingly, in order to upscale this concept to a size ranging from 50 to 100 MWe, the natural evolution would be to consider a different CSP technology, i.e., parabolic trough or solar tower, the second one being more adequate to enable higher temperatures at the turbine inlet, and hence having higher efficiencies. In such a case, sCO_2 power systems stem as one of the most promising solutions, given the higher efficiency of these cycles in comparison with conventional (steam) Rankine power cycles, which can bring about an important reduction in the land area occupied and, therefore, the capital expenditures (CAPEX) and levelised cost of electricity (LCoE) [11]. Finally, it is worth remarking that a CSP plant can be combined with thermal energy storage, thereby enabling the dispatchability of both power and water according to the needs of the end-user.

2. SOLMIDEFF Project

The main concept of SOLMIDEFF [10], a project funded by the Spanish National R+D+i Programme focused on societal challenges, is illustrated in Figure 1. A parabolic dish collector is used to collect and concentrate solar energy onto a focal plane where the power conversion unit (PCU) is installed. The PCU is comprised of a micro gas turbine engine (mGT) and a solar receiver. The compressor of the mGT swallows atmospheric air, which is compressed and fed into the solar receiver through the recuperative heat exchanger, which increases the temperature of this high-pressure air stream by harvesting the thermal energy of the hot gases flowing out from the turbine. The receiver is also a heat exchanger, which transfers the concentrated solar energy received from the collector to the incoming stream of pressurised air, delivering air at high pressure and temperature. This air, typically at around 800 °C, is then expanded across the turbine, where power is produced to drive both the compressor and the electric generator. The gases exhausting from the turbine are discharged to the atmosphere but, before this, they flow across a counter-current heat exchanger, where their thermal energy is used to preheat compressor delivery air before flowing into the solar receiver. The bottoming system of the SOLMIDEFF concept is comprised of two elements. An advanced desalination unit based on reverse osmosis technology is driven by the electric power produced by the micro gas turbine. This RO unit produces fresh water and a brine with a high concentration of salts that is treated

further in the second element of the bottoming system. This is a zero liquid discharge unit driven by the waste heat available in the exhaust of the micro turbine (air at some 250–300 °C), which evaporates a fraction of the water content in the brine, yielding a final brine with a higher concentration; therefore, it has lower environmental impact and is easier to handle.

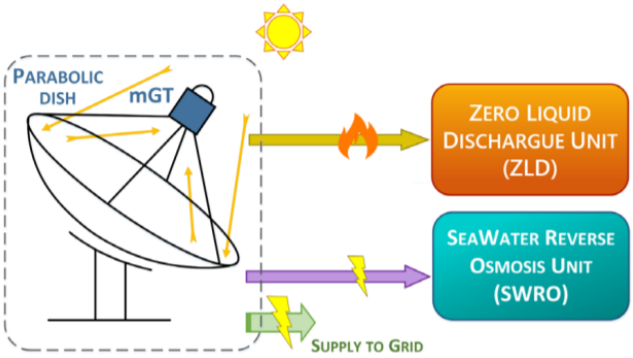

Figure 1. The SOLMIDEFF concept.

3. Supercritical CO_2 Power Cycles: History and Fundamentals of the Technology

The history of sCO_2 technology finds its roots in the independent but almost contemporaneous studies of Edward Feher [12] and Gianfranco Angelino [13–16] in the 1960s. Their seminal works lie within the general scope of closed-cycle gas turbine analysis, which had a significant interest in the second quarter of the XIX century, but focused on an innovative topic: thermodynamic cycles working near the critical point, employing carbon dioxide (and other innovative working fluids) as working fluid. On the one hand, Feher investigated the *simple recuperated* supercritical cycle (see Figure 2a) and performed a sensitivity assessment to the main operating parameters (maximum cycle temperature, minimum cycle temperature and minimum cycle pressure) as well as to the performance of the individual components (recuperator effectiveness, and turbomachinery isentropic efficiency). The reasons for considering supercritical CO_2 as alternative working fluid were, and remain, multiple: high thermal stability, low chemical reactivity, abundant in nature, non-flammable and inexpensive [17]. Nevertheless, its differential features are the critical temperature and pressure at 31.04 °C and 73.83 bar, respectively. This moderate value of temperature, very close to ambient, allows to perform the compression process near the critical point with conventional cooling systems, whilst the moderate critical pressure avoids mechanical requirements that are beyond what is practical with state-of-the-art technology. In the proximity of the critical point, a drastic decrease in specific volume occurs (Figure 3), resulting in a significant reduction in compression work when compared to other closed-cycle turbines using hot air or helium (Equation (1)).

$$W_c = \int_{in}^{out} v \cdot dp = \int_{in}^{out} Z \cdot \frac{R_g \cdot T}{P} \cdot dp \quad (1)$$

Further to the reduction of compression work, sCO_2 cycles are also characterised by a large heat recovery potential due to the high turbine outlet temperature, brought by the fairly low expansion ratios, which enhances thermal efficiency significantly [18]. Nevertheless, this potential is affected by one of the main downsides of the particular behaviour of CO_2 near the critical point (see Figure 3), where the large variations of physical properties with temperature trigger an *internal pinch-point* problem in the low temperature recuperator. Indeed, the significant heat capacity difference between the high and low pressure streams in the heat recuperator result in a minimum temperature difference that is found inside the heat exchanger instead of at one of its ends. The consequence is a higher irreversibility of the heat recovery process that eventually reduces the thermal efficiency of the cycle. In order to overcome this issue, Angelino proposed several advanced cycle layouts, capable of enhancing the thermal performance of the simple recuperative

cycle through the incorporation of two main strategies: the *split-flow compression* and the *pre-compression*.

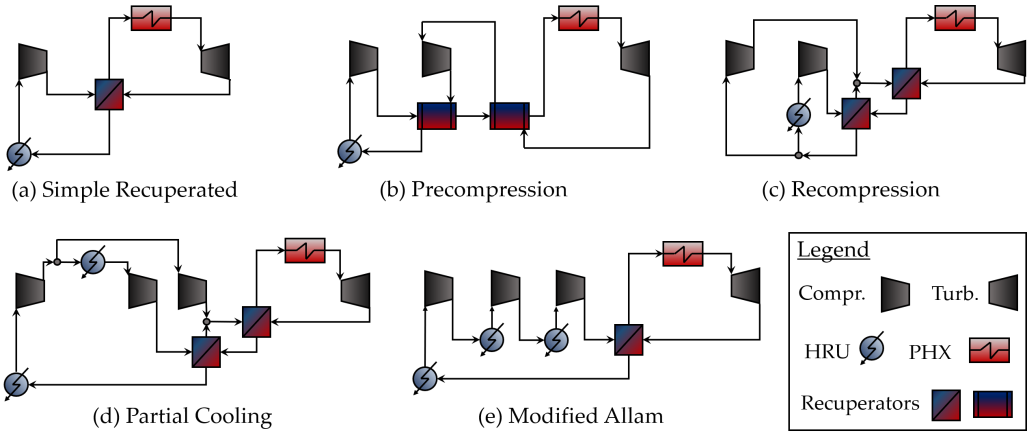

Figure 2. Summary of the five candidates supercritical CO_2 cycles studied.

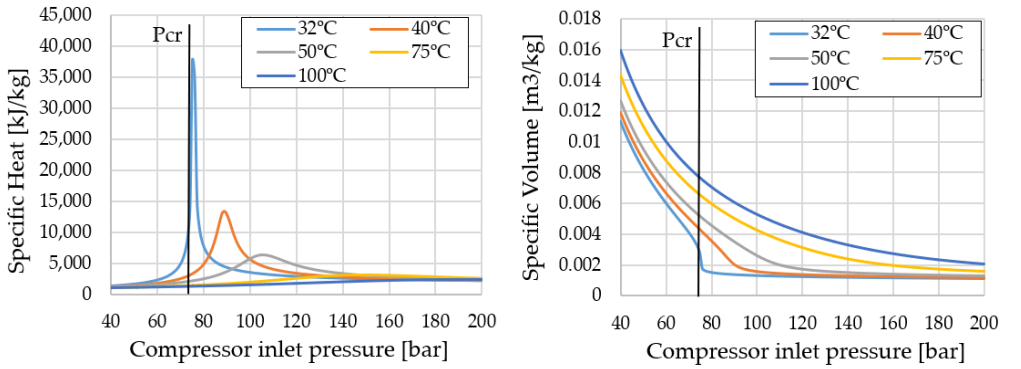

Figure 3. Trends of the thermo-physical properties of CO_2 in the vicinity of the critical point.

The *recompression* cycle is the most widespread supercritical CO_2 layout (Figure 2c). The heat recovery process is divided in two heat exchangers, a high-temperature recuperator (HTL) and a low-temperature recuperator (LTR). The flow in the low-pressure outlet of the LTR is also split in two: a fraction α is sent to the heat rejection unit (HRU) and the main compressor, whereas the remaining flow is directly compressed and mixed with the high-pressure outlet of the LTR. Thanks to this arrangement, the heat capacity of the high-pressure stream in the LTR can be reduced (reduction in the circulating mass flow), while the heat capacity of the low-pressure side remains the same. Even if cycle-specific work is reduced due to a higher compression power (a fraction of the flow is compressed far from the critical point), the thermal efficiency is considerably enhanced thanks to the higher effectiveness of the heat recuperators. A demonstration of this is provided by Figure 4, which shows that increasing the split flow factor (i.e., fraction of the mass flow that goes to the recompressor) significantly reduces the exergy destroyed in the heat recuperators at the expense of only of a small increase in exergy destruction across the compression and expansion processes. The amount of exergy destroyed in each cycle component is obtained using the correlation presented in Equation (2), making use of the concept of product exergy (E_P), fuel exergy (E_F) and exergy losses (E_L), k being a generic component. A thorough explanation of the methodology is available from the original paper by Penkhun and Tsatsaronis in [19], and it has already been employed by some of the authors in [20].

$$E_{D,k} = T_0 \Delta S_{gen,k} = E_{F,k} - E_{P,k} - E_{L,k} \quad (2)$$

The *pre-compression* layout makes use of a somewhat similar strategy to overcome the *internal pinch-point* issue thanks to a higher heat capacity of the low-pressure stream,

obtained thanks to a higher pressure. In this configuration, the recuperator is also divided in two different components, high and low temperature, and a compressor—namely, *precompressor*—is placed in the low-pressure line between the two of them (see Figure 2b). In this way, a twofold benefit can be achieved: a good balance between the heat capacities of the low and high pressure streams of the LTR, which significantly limits the *internal pinch-point* issue, and a further degree of freedom for optimisation because the turbine exhaust pressure can be varied independently from the inlet temperature to the main compressor.

Furthermore, it is worth remarking that these two strategies can be combined together, with the addition of a *pre-compression* right before the *split-flow compression*. The result is the so-called *partial cooling* cycle (see Figure 2d), originally proposed by Angelino in a transcritical scheme and nowadays widely considered one of the most promising layouts for sCO_2 power systems [11,21], due to its very good compromise between high thermal efficiency and high specific work.

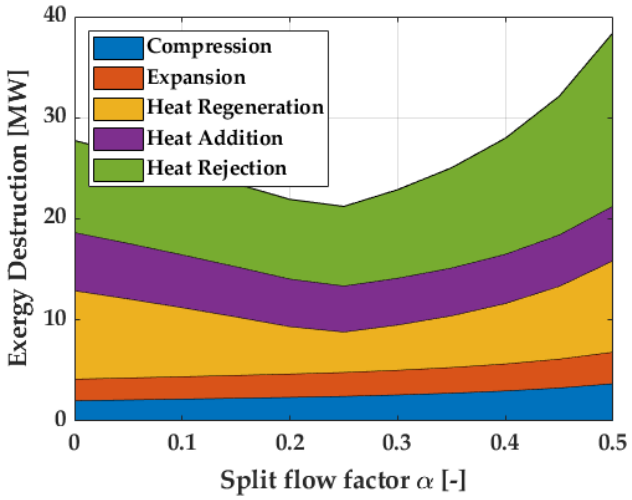

Figure 4. Changes in the profile of exergy destruction for a 50 MW_{th} system for variable split-flow factor.

In spite of these promising advanced layouts and the potential highlighted in the work by Feher and Angelino, the interest in sCO_2 technology decayed soon, owing to the development of combustion turbines and combined cycles. It was not until 2004, almost thirty-five years after, that sCO_2 technology drew the attention of the scientific community, thanks to Vaclav Dostal's doctoral dissertation developed at MIT [22]. Dostal studied the integration of advanced supercritical carbon dioxide cycles—*recompression* and *partial cooling*, in particular—with Generation IV nuclear applications, from thermodynamic and technological standpoints. This PhD thesis presented a critical review of the fundamentals established decades before by Angelino and Feher, setting up a landmark for the development of sCO_2 power systems. From this point on, an exponential growth of the interest in this technology was experienced, translated into a massive production of research papers and technical reports in which the potential of supercritical CO_2 power cycles was assessed for a number of different applications. In this regard, it is worth remarking the review papers developed by University of Seville [23] and City, University of London [1].

Nowadays, the technology is widely investigated by several European and American R&D programmes, as already commented in the introduction to this paper, and it is considered one of the most promising alternatives for various energy systems. Besides solar and nuclear applications, sCO_2 cycles have been investigated as well for waste heat recovery and fossil fuels through oxy-combustion systems. Actually, it is worth noting that there already exist commercial sCO_2 solutions for the latter application. First, an extremely compact waste heat recovery unit, employing a transcritical *simple recuperated*

cycle, was developed by Echogen [24]. Second, a major breakthrough in the oxy-combustion field—and sCO_2 in general—was achieved in 2019, when the first commercial large-scale (50 MW_{th}) oxy-combustion plant running on sCO_2 was started up in La Porte, Texas [25].

Combination of sCO_2 Cycles and CSP Plant

The combination of supercritical carbon dioxide power cycles and concentrated solar power plants was originally studied by the National Renewable Energy Laboratory [26–28], where researchers identified the *recompression* and the *partial cooling* cycles as the most promising configurations for next-generation CSP plants. From a techno-economic standpoint, the former stands out for its high thermal efficiency, which brings about a reduction in the cost of the solar field, but the latter yields a lower LCoE because its slightly lower efficiency is compensated for by a large reduction in the cost of the energy storage system [21]. These studies were also supported by the experimental tests conducted by SANDIA National Labs [29] and other small-scale facilities [30,31]. A further step was achieved by Crespi, who identified the best-performing layouts depending on boundary conditions (maximum and minimum cycle temperature) and carried out a preliminary techno-economic assessment of various layouts [32]. The work also concluded that the incorporation of reheat was not interesting in spite of the higher thermal efficiency, due to the higher capital costs.

Finding the optimal maximum operating temperature in a concentrated solar power system is a trade-off between power block efficiency and thermal losses of the receiver [33]. This can be seen in Figure 5 (left), where system efficiency, calculated as the product of solar receiver and power block efficiencies, is expressed as a function of the concentration ratio and receiver temperature. For solar tower technology, the concentration ratio is typically in the order of 1000, and thus the optimum receiver temperature is between 650 and 950 °C. It is in this region that the sCO_2 cycle outperforms the Rankine cycle and gas turbine, as seen in Figure 5 (right).

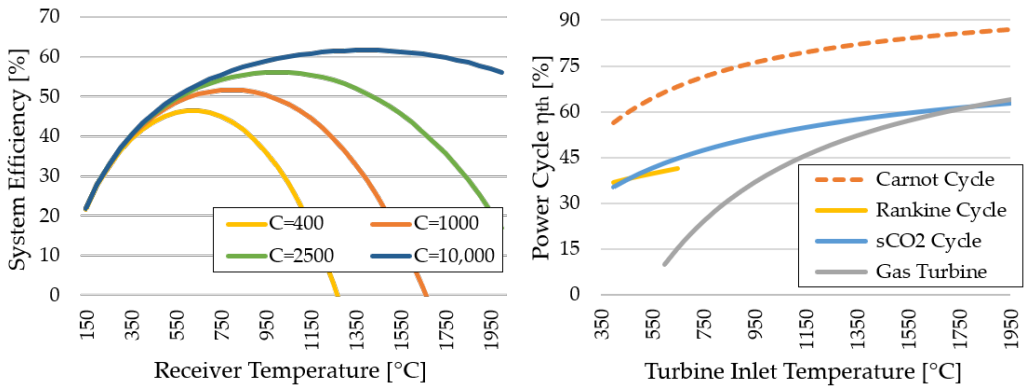

Figure 5. System efficiency of a concentrated solar power plant as a function of solar receiver temperature and concentration ratio (**left**) and power block thermal efficiency as a function of turbine inlet temperature for various power cycle technologies (**right**).

A final comment about the influence of ambient temperature is mandatory: sCO_2 cycles are very sensitive to changes in the minimum cycle temperature. As this temperature rises, the benefits of performing the compression near the critical point are lost, as achieving such low temperatures is no longer possible; as a consequence, thermal efficiency drops by 2 to 4 percentage points when moving from 35 °C to 50 °C for the most common cycle topologies [34]. Moreover, concentrated solar power plants are usually located in arid regions with high direct normal irradiance (DNI) and ambient temperatures, and with low availability of cooling water. This makes working near the critical point even more difficult, though, at the same time, it paves the way for significant performance enhancements if a low temperature system making use of waste thermal energy from the power generation cycle could be incorporated.

4. Computational Environment

Five different power cycles are considered, identified in previous works by some of the authors of this work [35]: *simple recuperated*, *precompression*, *recompression*, *partial cooling* and *modified Allam*. These four configurations were already discussed in the previous section and their layouts are provided in Figure 2. On the other hand, the *modified Allam* cycle is a modification of *Allam* adapted to operation on pure-CO_2 embodiment (without oxy-combustion), and basically consists of a *simple recuperated* cycle enhanced with a two-stage intercooling (see Figure 2a,e).

The entire set of cycles is modelled with the commercial software Thermoflex [36], considering a rated net power output of 50 MW_e. The maximum cycle pressure is set to 250 bar, which is found to be a cost-effective value in the literature [21]. Turbomachinery is modelled through a constant isentropic efficiency of 92% and 89% for turbines and compressors, respectively. The heat recuperators are modelled, setting the pinch point (i.e., minimum temperature difference) to 5 °C. Finally, pressure losses are 1.5% in the high pressure side and 1.0% in the low pressure side. The boundary conditions are summarised in Table 1.

Table 1. Set of boundary conditions for sCO_2 power cycles.

Component	Parameter	Reference Value
Turbine	Isentropic efficiency	92%
Compressor	Isentropic efficiency	89%
Heat Recuperator	Pinch Point	5 °C
Heat Recuperator	Pressure Losses (High Pressure side)	1.5%
Heat Recuperator	Pressure Losses (Low Pressure side)	1.0%
Primary Heat Exchanger	Pressure Losses (CO_2 side)	1.5%
Heat Rejection Unit	Pressure Losses (CO_2 side)	1.0%

Two turbine inlet temperatures are considered: 550 °C and 700 °C. The former is representative of state-of-the-art CSP technology, whereas the latter is the target for advanced CSP plants. Additionally, two minimum cycle temperatures are studied: 35 °C (mild climate regions) and 50 °C (semi-arid regions). The remaining operating parameters of each cycle are optimised for the four boundary conditions dataset by means of the *SurrogateOpt* function in MatLab's Optimisation Toolbox, which is recommended for highly time-consuming objective functions as the simulation of supercritical power cycles [37].

The reverse osmosis system is modelled using LG Q+ v2.4 software [38]. The membranes employed are 440 ft^2 from LG (SR,GR,R,ES). Two locations are selected, *Santa Cruz de Tenerife* and *Abu Dhabi*, representative of mild and semi-arid locations, respectively. Seawater compositions are obtained from Wilf [39] and described in Table 2. In the Persian Gulf case, the upper bound for seawater temperature is selected for the design case since fresh water quality is harder to obtain at high temperatures.

Table 2. Seawater composition (data from [39]).

Constituent	Canary Islands	Persian Gulf
Temperature [°C]	22	16–34
pH	7.8	7.0
Boron [ppm]	4.5	5
TDS [ppm]	38,739	45,199

5. Results and Discussion

The first step of this research is the thermodynamic optimisation of the five candidate sCO_2 power cycles, considering thermal efficiency as the main figure of merit. More information regarding optimisation can be found in a previous work by the authors [34]. Figure 6 shows the results as a function of minimum and maximum cycle temperatures

(i.e., four possible combinations of the boundary conditions discussed above). An evident trend is that the *recompression* cycle has the best performance in all cases, closely followed by *partial cooling*, then the *precompression* cycle, with a thermal efficiency that is roughly 1.5 percentage points lower, followed by *modified Allam* and, finally, *simple recuperated*. If locations with mild temperatures are considered (T_{min} = 35 °C), the actual potential of the sCO_2 power cycles can be estimated at 46.3%, for state-of-the-art CSP plants (TIT = 550 °C) and 52.8% for advanced ones (TIT = 700 °C). On the other hand, for semi-arid locations, the maximum achievable thermal efficiency drops to 42.4% and 49.2%, respectively.

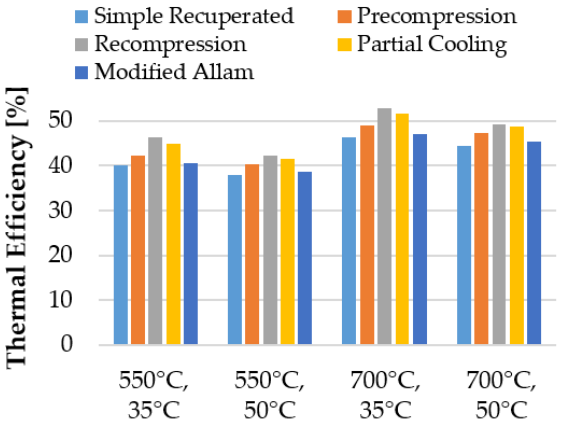

Figure 6. Thermal efficiency of the sCO_2 configurations studied, for different boundary conditions.

Once thermal performance and operating conditions of the different sCO_2 systems are assessed, the integration with desalination is analysed. To this end, Figure 7 shows the temperature at which heat is rejected from each cycle, a key parameter to assess the feasibility of thermal desalination. Regarding the *recompression* cycle, the inlet temperature of the heat rejection temperature rises with both T_{min} and TIT, with a stronger dependence on the former. At 35 °C, for both values of TIT, the inlet to the HRU is at around 80 °C, while it increases to 102–108 °C at 50 °C. The two configurations incorporating a precompressor, *precompression* and *partial cooling*, present very low inlet temperature to the HRU (around 60–80 °C), which in turn varies randomly with boundary conditions. The *simple recuperated* and *modified Allam* cycles exhibit the highest HRU inlet temperatures, with values higher than 100 °C at 550 °C/35 °C and around 140 °C at 700 °C/50 °C.

Whether or not these temperatures are suitable for multi-effect distillation (MED) or membrane distillation (MD) systems is a matter of discussion. The heat input to commercial MED/MD systems is usually in the form of saturated steam, which should be kept at a temperature higher than 90 °C in order to obtain a good performance ratio (PR), around 10 for MED and 13.5 for MD. For lower temperatures, a dramatic performance drop is observed [9]. Based on this, and setting a lower threshold of this temperature at 90 °C, only the *recuperated Rankine* and the *modified Allam* could be employed to supply heat to the MED/MD plant, and this with poor results. As a matter of fact, only a small fraction of the sensible heat could be used for desalination, harvesting the thermal energy available in the working fluid from the temperature in Figure 7 to 93 °C (considering a 3 °C approach); the remaining waste heat should still have to be rejected from the cycle via HRU. From here, it becomes evident that only a very small amount of fresh water could be produced, yielding little interest in the integration between sCO_2 power cycles and conventional distillation technologies.

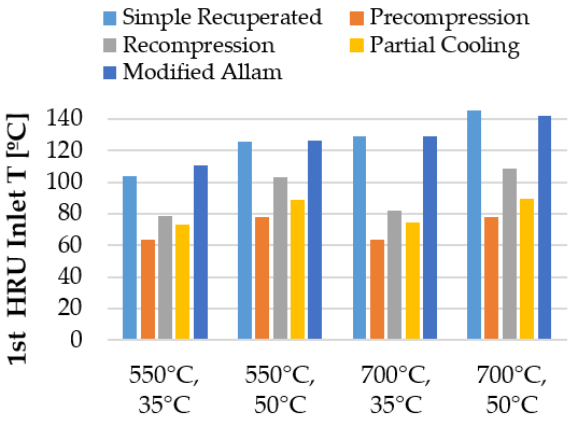

Figure 7. Inlet temperature to the first heat rejection unit of the sCO_2 configurations studied, for different boundary conditions.

In the third step of the present paper, reverse osmosis systems are considered. Employing the software Q+, a reverse osmosis system is designed for each reference location, making use of a standard general two-pass configuration with a 45% recovery rate in the first pass. The number of pressure vessels is determined in order to achieve an average flux of 14.5 L/m^2· h with only one stage. The flux in the first element must not exceed 1.1 m^2/h in order to reduce fouling (i.e., reduce maintenance cost). The second pass has two stages, with a total recovery rate of 90%. The number of pressure vessels must ensure an average flux of 31 L/m^2· h and be arranged with a 2:1 ratio between the first and second stages. The two-pass configuration includes pH adjustment between passes as well as bypass of the second pass. Pump efficiency is set to 80%, which is a conservative value. The energy carried by the brine of the first pass is recovered using an Isobar Chamber with 0.7 bar pressure difference, 5% mixing and 0% leakage. All pressure vessels are comprised of 7 elements. Finally, the fresh water quality must be below 1 ppm in *Santa Cruz de Tenerife* [40] and 1.5 ppm in *Abu Dhabi* [41]. A limit in the total dissolved solids (TDS) is not explicitly specified, for the boron restriction is restrictive enough to ensure a low value of TDS. These design criteria are summarised in Table 3.

Table 3. Design criteria of the seawater reverse osmosis plant modelled with Q+.

Parameter	Reference Value
Recovery rate (first pass)	45%
Average flux—first pass	14.5 L/m^2·h
Maximum flux allowable (first pass)	1.1 m^3/h
Number of stages (first pass)	1
Recovery rate (second pass)	90%
Average flux—second pass	31 L/m^2·h
Number of stages (second pass)	2 (2:1 vessels)
pH adjustment between passes	Yes
Bypass of second pass	Yes
Pump efficiency	80%
Isobaric chamber specs	0.7 bar pressure difference, 5% mixing, 0% leakage
Number of elements per vessel	7 elements
Boron concentration-freshwater	1 ppm (*Santa Cruz de Tenerife*) 1.5 ppm (*Abu Dhabi*)

The design methodology employed can be described as follows. First, single-pass configurations are explored. If the fresh water quality restrictions can be achieved with the model with highest salt rejection, hybrid membrane inter-stage designs (HID) are studied, following the criteria from [42]. HID enables to reduce the operating pressure (thus the

specific energy consumption) as well as balancing the flux among the elements of the pressure vessels. If one pass is not enough, a second pass with double stage is incorporated.

Results are indicated in Table 4. For *Santa Cruz de Tenerife* (mild climate location), a single-pass configuration can achieve the desired quality. A HID combining (2)440SR, (2)440GR and (3)440ES models is selected in order to approximate the boron quality to the threshold value of 1 ppm, as well as to reduce the flux in the first element below 1.04 m^3/h. As a consequence, the operating pressure is reduced to 58.2 bar and the resulting SEC is 2.16 kWh/m^3. The higher value of the boron restriction in *Abu Dhabi* (semi-arid location) enables also a single-pass configuration. A HID design using (1)440SR, (1)440GR and (5)440R is found to obtain 1.50 ppm of boron with an operating pressure of 66.4 bar, though the average flux has to be reduced to 12.6 $L/m^2 \cdot h$ in order to keep the flux in the first element below the limit reported in Table 3. The resulting SEC of the *Abu Dhabi* configuration is 2.44 kWh/m^3. Finally, the concentration of TDS is 212 ppm for *Santa Cruz de Tenerife* and 395 ppm for *Abu Dhabi*, both of them acceptable values [43].

Table 4. Seawater reverse osmosis (SWRO) reference plant for *Santa Cruz de Tenerife* and *Abu Dhabi*.

	Santa Cruz de Tenerife	***Abu Dhabi***
Membranes (first pass)	(2)440SR, (2)440GR, (3)440ES	(1)440SR, (1)440GR, (5)440R
Boron concentration [ppm]	0.98	1.50
TDS concentration [ppm]	212.33	394.8
Average flux [$L/m^2 \cdot h$]	14.3	12.6
First element flux [m^3/h]	1.04	1.1
Operating pressure [bar]	58.2	66.4
Total recovery rate [%]	45	45
SEC [kWh/m^3]	2.16	2.44
SEC auxiliaries [kWh/m^3]	0.75	0.75
Total SEC [kWh/m^3]	2.91	3.19

The calculated SEC value—including 0.75 kWh/m^3 to account for auxiliaries—can be combined with the thermodynamic results of the sCO_2 cycle to determine the specific energy consumption (in kJ/kg) of the solar desalination technology by means of Equation (3). The solar-to-electric efficiency of the CSP tower plant is obtained by merely multiplying the thermal efficiency in Figure 6 by the combined efficiency of solar field and receiver, set to 60% and 90%, respectively, and by the mechanical efficiency of the turbogenerator arrangement, set to 94%. The final value of the solar-to-electric efficiency is, therefore, case specific, depending on the cycle configuration and boundary conditions considered, and it ranges from 20% to 26%. The RO SEC depends only on the minimum temperature considered, and the density of fresh water is approximated to that of pure water at the feed temperature.

$$\mathrm{SEC}\left[\frac{\mathrm{kJ}}{\mathrm{kg}}\right] = \frac{SEC_{RO}\left[\frac{\mathrm{kWh}}{\mathrm{m}^3}\right] \cdot 3600 \frac{\mathrm{kJ}}{\mathrm{kWh}} \cdot \frac{1}{\rho_{\mathrm{product}}\left[\frac{\mathrm{kg}}{\mathrm{m}^3}\right]}}{\eta_{\text{solar-to-electric}}} \quad (3)$$

The results in Figure 8 show very good prospects for solar desalination coupling RO to sCO_2 power cycles. The high thermal efficiency of these cycles together with a tailored design of the reverse osmosis system enables an energy cost per kg of fresh water as low as 39.29 kJ/kg. For the sake of comparison, the SEC using photovoltaics (PV) driven RO is also calculated, assuming a 18% solar-to-electric efficiency of the photovoltaic panels. For the four scenarios, the sCO_2 technology yields similar SEC to that of PV, driven by the high thermal efficiency of supercritical power cycles.

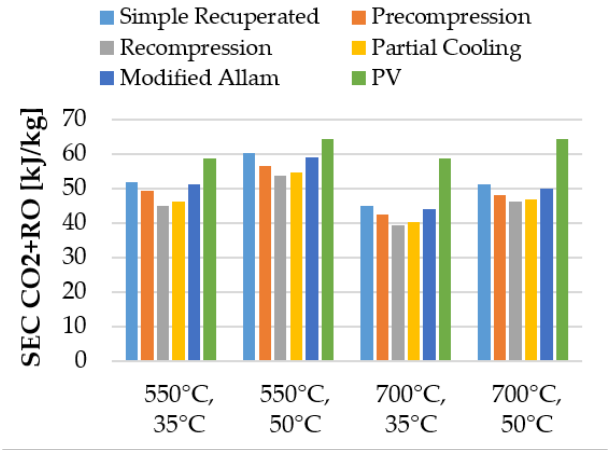

Figure 8. Specific energy consumption [kJ/kg] of fresh water desalination using sCO_2 power cycles and reverse osmosis (including 0.75 kWh/m^3 auxiliary power consumption). Green bars correspond to PV-RO systems with 18% solar-to-electric efficiency.

One consequence of the higher solar-to-electric efficiency of sCO_2 power cycles against PV is a reduction in the effective area of the solar field. Considering a Direct normal irradiance (DNI) of 800 W/m^2, the PV plant requires an aperture area of 347,222 m^2 (i.e., surface of the solar panels), as compared to 232,988 m^2 for the solar field required by a sCO_2 system running on a *recompression* cycle in the most advantageous conditions. In other words, employing a high-thermal efficiency sCO_2 would enable a reduction of about 110,000 m^2 of collector with respect to PV.

Moreover, the share of electric power demanded by the RO plant—with respect to 50 MW_e—is assessed for the cases under analysis and presented in Table 5, considering two possible scenarios: 1% and 30% share (percentage of total electricity generation that is used to produce fresh water). The former allows a fresh water production of around 3700–4100 m^3/day, depending on the location considered, enough to cover the water supply of medium-size communities without industry. The latter achieves water productions higher than 110,000 m^3/day.

Table 5. Water production in m^3/day.

Power Share	*Santa Cruz de Tenerife*	*Abu Dhabi*
1%	4124 m^3/day	3762 m^3/day
30%	123,711 m^3/day	112,853 m^3/day

Finally, it is worth noting that the specific energy consumption could be further reduced if the heat rejected from the cycles is used to decrease the power consumption of the RO unit. To that end, the strategy of preheating the feed water stream is explored. The effectiveness of the strategy is studied separately for each reference plant. For *Santa Cruz de Tenerife*, the feed water temperature is increased from 22 °C (design case) to 40 °C, but this brings about a negligible SEC reduction from 2.91 kWh/m^3 to 2.83 kWh/m^3 according to Figure 9. In addition, the quality of the permeate water deteriorates significantly, exceeding the allowable concentration of boron. Moreover, the adoption of specific designs to increase the rejection of salt from the pressure vessels at each temperature level completely offsets the SEC reduction obtained from the preheating of feed water. For such reasons, the preheating strategy (i.e., increasing temperature with respect to design temperature) is not recommended for plants where the design is driven by the quality of fresh water.

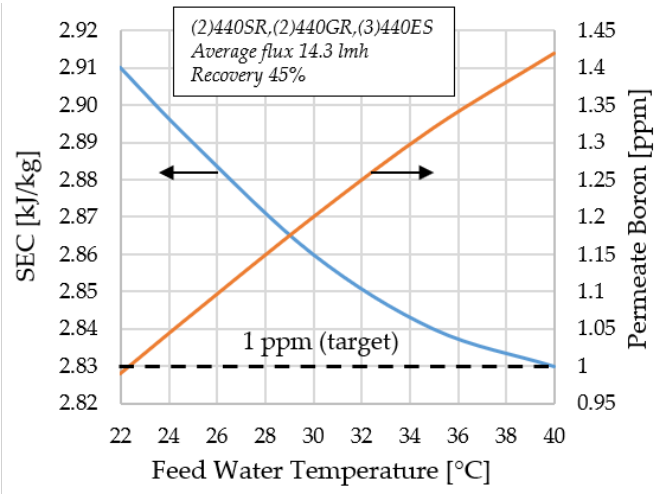

Figure 9. Influence of feed water temperature in *Santa Cruz de Tenerife*. Sea water composition from Table 2.

The Persian Gulf case yields a different situation. According to Wilf [39], the sea water temperature oscillates from 16 °C to 34 °C over the year. The influence of temperature on SEC and on the concentration of boron in the product in the plant located in the Persian Gulf is illustrated in Figure 10. Again, achieving temperatures higher than the design value are not interesting for the exact same effect on product quality. On the other hand, a significant SEC increase from 3.19 kWh/m^3 to 3.32 kWh/m^3 (4%) is experienced when the temperature of feed water temperature drops to the lower bound of 16 °C. It is true that, in these conditions, the waste heat from the sCO_2 cycle could be used to increase the feed water temperature to the design value (34 °C); nevertheless, the maximum improvement attainable is limited to 0.13 kWh/m^3 for the coldest days in the year, thus compromising the cost effectiveness of such a preheating strategy. A thorough techno-economic assessment on an annual yield basis is here mandatory.

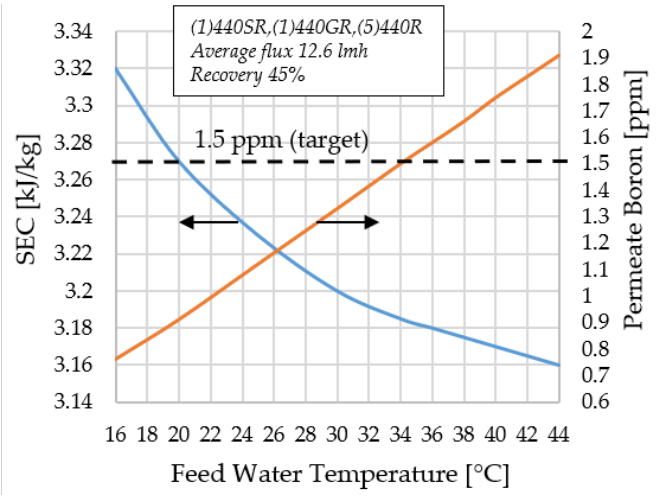

Figure 10. Influence of feed water temperature in the Persian Gulf. Sea water composition from Table 2.

6. Conclusions

This paper investigated the potential of sCO_2 power cycles for solar desalination, as a possible power generation technology supporting the upscaling of the concept proposed by the SOLMIDEFF project. Five different cycles were considered: *simple recuperated*, *precompression*, *recompression*, *partial cooling* and *modified Allam*, which are identified in the literature as the most interesting configurations. Two different minimum cycle temperatures were studied, 35 °C and 50 °C, representative of two reference locations in desalination analyses,

Santa Cruz de Tenerife and *Abu Dhabi*, respectively. Similarly, two turbine inlet temperatures were considered: 550 °C, corresponding to the state-of-the-art solar towers, and 700 °C, representative of next-generation CSP plants with central receiver technology.

The results showed that the *recompression* cycle achieves the highest thermal efficiency in the four sets of boundary conditions studied, closely followed by *partial cooling*. Moreover, all the cycles under analysis present a fairly low temperature at the inlet to the heat rejection unit, generally lower than 100 °C. This is an interesting feature to achieve high thermal efficiency, but in distillation systems, a high heat rejection unit inlet temperature is required to produce saturated steam. Thus, it is concluded that the available temperatures at the cooling system of the sCO_2 cycle are too low to integrate MED/MD systems efficiently. For these reasons, reverse osmosis systems were studied instead.

To carry out such analysis, the paper showed the design of a SWRO plant, adapted to each location, using Q+ software. This resulted in a specific energy consumption of 2.91 and 3.19 kWh/m^3 respectively, accounting for the RO unit only. The specific energy consumption of the overall solar-to-water process, in kJ/kg, when using integrated sCO_2 cycles and RO is also calculated and compared to the reference case comprised of photovoltaic panels plus reverse osmosis (PV+RO). The results showed that the higher solar-to-electric efficiency of the sCO_2 cycle leads to a lower global SEC than PV+RO, with values as low as 39.3 kJ/kg (for a CSP plant running on a sCO_2 *Recompression* cycle at 700/35 °C).

For the sake of completeness, a further modification based on harvesting the available waste heat from the cycle to preheat the feed water stream of the RO unit was also investigated. From the results obtained, it is concluded that the most promising integration between sCO_2 and RO does not incorporate such a solution, and that the preheating may be interesting in scenarios where water quality is not a concern, for instance, locations with more permissive water regulation that does not limit the design of the RO plant (e.g., Canada or Australia) or the retrofitting of existing RO installations that still have a margin to increase the concentration of boron in the product.

Finally, it is worth mentioning that the cooling of sCO_2 cycles is by no means a minor issue. Air cooling, as usually proposed in the literature, involves higher minimum cycle temperatures, which have a strong negative effect on thermal efficiency and increase the overall footprint and auxiliary power consumption of the plant with respect to wet cooling. Accordingly, future studies must focus on the beneficial utilisation of water for desalination as heat transfer fluid in the heat rejection units, looking for beneficial effects on cycle performance and not so much a positive impact on water production. Similarly, future studies must also investigate the possible integration of zero liquid discharge systems in an upscaled SOLMIDEFF concept.

Author Contributions: Conceptualisation: R.G.-A., P.R.d.A. and F.C.; methodology, P.R.d.A. and R.G.-A.; software, P.R.d.A. and R.G.-A.; investigation, P.R.d.A. and R.G.-A.; data curation, R.G.-A. and A.M.; writing—original draft preparation, P.R.d.A. and R.G.-A.; writing—review and editing, F.C., D.S. and T.S.-L.; supervision, F.C. and D.S. All authors have read and agreed to the published version of the manuscript.

Funding: This manuscript has been developed in the framework of SOLMIDEFF project, under grant agreement RTI2018-102196-B-100, funded by MCIN/AEI/10.13039/501100011033 and by "ERDF A way of making Europe". This research was also supported by University of Seville through the Internal Research Programme (Plan Propio de Investigación), under contract No 2019/00000359. Finally, the regional government of Andalusia (Junta de Andalucía) is gratefully acknowledged for sponsoring the contract of Pablo Rodríguez de Arriba under the Programme for Youth Employment 2014–2020-Phase 4 (Plan de empleo de garantía juvenil-Fase 4).

Conflicts of Interest: The authors declare no conflict of interest.

Abbreviations

The following abbreviations are used in this manuscript:

α	Split-flow Factor
η	Efficiency
C	Concentration Ratio
CAPEX	Capital Expenditures
CSP	Concentrated Solar Power
DNI	Direct Normal Irradiance
HID	Hybrid Membrane Inter-stage Designs
HTR	High-Temperature Recuperator
HRU	Heat Rejection Unit
LCoE	Levelised Cost of Electricity
LTR	Low-temperature Recuperator
MD	Membrane Distillation
MED	Multi-effect Distillation
mGT	Micro Gas Turbine
PCU	Power Conversion Unit
PHX	Primary Heat Exchanger
PR	Performance Ratio
PV	Photovoltaics
RO	Reverse Osmosis
SEC	Specific Energy Consumption
TDS	Total Dissolved Solids
TIT	Turbine Inlet Temperature
T_{min}	Minimum Cycle Temperature

References

1. White, M.T.; Bianchi, G.; Chai, L.; Tassou, S.A.; Sayma, A.I. Review of supercritical CO_2 technologies and systems for power generation. *Appl. Therm. Eng.* **2021**, *185*, 116447. [CrossRef]
2. SCARABEUS Project: Supercritical CARbon Dioxide/Alternative Fluid Blends for Efficiency Upgrade of Solar Power Plants. Grant ID: 814985. Available online: https://cordis.europa.eu/project/id/814985 (accessed on 26 October 2021).
3. COMPASsCO2 Project: COMponents' and Materials' Performance for Advanced Solar Supercritical CO_2 Power Plants. Grant ID: 958418. Available online: https://cordis.europa.eu/project/id/958418 (accessed on 26 October 2021).
4. sCO2-Flex Project: Supercritical CO_2 Cycle for Flexible and Sustainable Support to the Electricity System. Grant ID: 764690. Available online: https://cordis.europa.eu/project/id/764690 (accessed on 26 October 2021).
5. sCO2-4-NPP Project: Innovative sCO_2-Based Heat Removal Technology for an Increased Level of Safety of Nuclear Power Plants. Grant ID: 847606. Available online: https://cordis.europa.eu/project/id/847606 (accessed on 26 October 2021).
6. sCO2-Hero Project: The Supercritical CO_2 Heat Removal System. Grandt ID: 662116. Available online: https://cordis.europa.eu/project/id/662116 (accessed on 26 October 2021).
7. I-ThERM Project: Industrial Thermal Energy Recovery Conversion and Management. Grandt ID: 680599. Available online: https://cordis.europa.eu/project/id/680599 (accessed on 26 October 2021).
8. CO2OLHEAT Project: Supercritical CO_2 Power Cycles Demonstration in Operational Environment Locally Valorising Industrial Waste Heat. Grandt ID: 101022831. Available online: https://cordis.europa.eu/project/id/101022831 (accessed on 26 October 2021).
9. Pouyfaucon, A.B.; García-Rodríguez, L. Solar thermal-powered desalination: A viable solution for a potential market. *Desalination* **2018**, *435*, 60–69. [CrossRef]
10. SOLMIDEFF Project: SOLar Micro Gas Turbine-Driven Desalination for Environmental oFF-Grid. 2019. Available online: http://institucional.us.es/solmideff/index.html (accessed on 6 December 2021).
11. Crespi, F.; Sánchez, D.; Martínez, G.S.; Sánchez-Lencero, T.; Jiménez-Espadafor, F. Potential of supercritical carbon dioxide power cycles to reduce the levelised cost of electricity of contemporary concentrated solar power plants. *Appl. Sci.* **2020**, *10*, 5049. [CrossRef]
12. Feher, E.G. The supercritical thermodynamic power cycle. *Energy Convers.* **1968**, *8*, 85–90. [CrossRef]
13. Angelino, G. Perspective for the Liquid Phase Compression Gas Turbine. *J. Eng. Gas Turbines Power* **1967**, *89*, 229–236. [CrossRef]
14. Angelino, G. Liquid-phase compression gas turbine for space power applications. *J. Spacecr. Rocket.* **1967**, *4*, 188–194. [CrossRef]
15. Angelino, G. Carbon Dioxide Condensation Cycles for Power Production. *J. Eng. Power* **1968**, *90*, 287–295. [CrossRef]
16. Angelino, G. Real Gas Effects in Carbon Dioxide Cycles. In Proceedings of the Turbo Expo: Power for Land, Sea, and Air, Cleveland, OH, USA, 9–13 March 1969.

17. Pierantozzi, R. Carbon Dioxide. In *Kirk-Othmer Encyclopedia of Chemical Technology*; John Wiley and Sons: New York, NY, USA, 2003.
18. Gülen, S.C. Supercritical CO_2—What Is It Good For? In *Gas Turbine World*; Pequot Publishing Inc.: Southport, CT, USA, 2016.
19. Penkuhn, M.; Tsatsaronis, G. Systematic Evaluation of Efficiency Improvement Options for sCO_2 Brayton Cycles. *Energy* **2020**, *210*, 118476. [CrossRef]
20. Crespi, F.; Rodríguez de Arriba, P.; Sánchez, D.; Muñoz, A.; Sánchez, T. The Potential of Supercritical Cycles Based on CO_2 Mixtures in Concentrated Solar Power Plants: An Exergy-Based Analysis. In Proceedings of the 6th International Seminar on ORC Power Systems, Munich, Germany, 11–13 October 2021.
21. Neises, T.; Turchi, C. Supercritical carbon dioxide power cycle design and configuration optimization to minimize levelized cost of energy of molten salt power towers operating at 650 °C. *Sol. Energy* **2019**, *181*, 27–36. [CrossRef]
22. Dostal, V. A Supercritical Carbon Dioxide Cycle for Next Generation Nuclear Reactors. Ph.D. Thesis, Massachusetts Institute of Technology, Cambridge, MA, USA, 2004.
23. Crespi, F.; Gavagnin, G.; Sánchez, D.; Martínez, G.S. Supercritical Carbon Dioxide Cycles for Power Generation: A Review. *Appl. Energy* **2017**, *195*, 152–183. [CrossRef]
24. Persichilli, M.; Held, T.; Hostler, S.; Zdankiewicz, E.; Klapp, D. Transforming Waste Heat to Power Through Development of a CO_2-Based Power Cycle. In Proceedings of the Electric Power Expo 2011, Rosemount, IL, USA, 10–12 May 2011; pp. 1–9.
25. NET Power's Clean Energy Demonstration Plant, La Porte, Texas. Available online: https://www.power-technology.com/projects/net-powers-clean-energy-demonstration-plant-la-porte-texas/ (accessed on 26 October 2021).
26. Turchi, C.S.; Ma, Z.; Dyreby, J. Supercritical Carbon Dioxide Power Cycle Configurations for use in Concentrating Solar Power Systems. In Proceedings of the Turbo Expo: Power for Land, Sea, and Air, Copenhagen, Denmark, 11–15 June 2012.
27. Turchi, C.S.; Ma, Z.; Neises, T.W.; Wagner, M.J. Thermodynamic study of advanced supercritical carbon dioxide power cycles for concentrating solar power systems. *J. Sol. Energy Eng.* **2013**, *135*, 041007. [CrossRef]
28. Neises, T.; Turchi, C. A comparison of supercritical carbon dioxide power cycle configurations with an emphasis on CSP applications. *Energy Procedia* **2014**, *49*, 1187–1196. [CrossRef]
29. Wright, S.A.; Radel, R.F.; Conboy, T.M.; Rochau, G.E. Modeling and Experimental Results for Condensing Supercritical CO_2 Power Cycles. Sandia Technical Report. 2011. Available online: https://www.researchgate.net/profile/Gary-Rochau/publication/241972169_Modeling_and_experimental_results_for_condensing_supercritical_CO2_power_cycles/links/57e1874e08ae9e25307d3e30/Modeling-and-experimental-results-for-condensing-supercritical-CO2-power-cycles.pdf (accessed on 27 October 2021).
30. Kimball, K.J.; Clementoni, E.M. Supercritical carbon dioxide Brayton power cycle development overview. In Proceedings of the Turbo Expo: Power for Land, Sea, and Air, Copenhagen, Denmark, 11–15 June 2012.
31. Cho, J.; Shin, H.; Ra, H.S.; Lee, G.; Roh, C.; Lee, B.; Baik, Y.J. Development of the supercritical carbon dioxide power cycle experimental loop in KIER. In Proceedings of the Turbo Expo: Power for Land, Sea, and Air, Seoul, Korea, 13–17 June 2016.
32. Crespi, F. Thermo-Economic Assessment of Supercritical CO_2 Power Cycles for Concentrated Solar Power Plants. Ph.D. Thesis, University of Seville, Seville, Spain, 2020.
33. Lovegrove, K.; Stein, W. (Eds.) *Concentrating Solar Power Technology: Principles, Developments and Applications*, 2nd ed.; Elsevier: Amsterdam, The Netherlands, 2020.
34. Crespi, F.; de Arriba, P.R.; Sánchez, D.; Ayub, A.; Di Marcoberardino, G.; Invernizzi, C.M.; Martínez, G.S.; Iora, P.; Di Bona, D.; Binotti, M.; et al. Thermal efficiency gains enabled by using CO_2 mixtures in supercritical power cycles. *Energy* **2022**, *238*, 121899. [CrossRef]
35. Crespi, F.; Sánchez, D.; Sánchez, T.; Martínez, G.S. Capital cost assessment of concentrated solar power plants based on supercritical carbon dioxide power cycles. *ASME J. Eng. Gas Turbines Power* **2019**, *141*, 071011. [CrossRef]
36. Thermoflow Inc. Thermoflow Suite—Thermoflex Software v.29. 2020. Available online: https://www.thermoflow.com/products_generalpurpose.html (accessed on 27 October 2021).
37. MathWorks, Surrogate Optimization. Available online: https://es.mathworks.com/help/gads/surrogate-optimization.html (accessed on 27 October 2021).
38. LG Chem—Water Solutions; Software Q+ v 2.4. Available online: https://www.lgwatersolutions.com/en/tools/software (accessed on 27 October 2021).
39. Wilf, M.; Awerbuch, L. *The Guidebook to Membrane Desalination Technology: Reverse Osmosis, Nanofiltration and Hybrid Systems: Process, Design, Applications and Economics*; Balaban Desalination Publications: Hopkinton, MA, USA, 2007.
40. Real Decreto 140/2003, de 7 de febrero, por el que se establecen los criterios sanitarios de la calidad del agua de consumo humano. Available online: https://www.boe.es/buscar/act.php?id=BOE-A-2003-3596 (accessed on 29 October 2021).
41. Tu, K.L.; Nghiem, L.D.; Chivas, A.R. Boron removal by reverse osmosis membranes in seawater desalination applications. *Sep. Purif. Technol.* **2010**, *75*, 87–101. [CrossRef]
42. Peñate, B.; García-Rodríguez, L. Reverse osmosis hybrid membrane inter-stage design: A comparative performance assessment. *Desalination* **2011**, *281*, 354–363. [CrossRef]
43. Guidelines for Drinking-Water Quality, 4th Edition, Incorporating the 1st Addendum. Available online: https://www.who.int/publications/i/item/9789241549950 (accessed on 29 October 2021).